ARCHIVES OF ELECTRICAL ENGINEERING VOL. 69(4), pp. 857–872 (2020)

DOI 10.24425/aee.2020.134635

Effect of polarized signals on the performance of adaptive antenna arrays

AMIN H. AL KA'BI

Australian College of Kuwait,
Kuwait
e-mail: a.kabi@ack.edu.kw

(Received: 25.01.2020, revised: 08.05.2020)

Abstract: The polarized electromagnetic waves have significant impact on the performance of adaptive antenna arrays. In this paper we investigate the effect of polarized desired and undesired signals on the performance of electronically steered beam adaptive antenna arrays. To achieve this goal, we built an analytical signal model for the adaptive array, in order to analyze, and compare the effect of polarized signals on the output SINRs (signal to interference plus noise ratios) of single-dipole, and cross-dipole adaptive antenna arrays. Based on a proof-of-concept experiment, and on MATLAB simulation results, it will be shown that cross-dipole adaptive antenna arrays exhibit better performance in comparison with single-dipole adaptive antenna arrays in presence of randomly polarized signals. However, single-dipole arrays show better performance under certain operating conditions.

Key words: adaptive arrays, antennas, electromagnetics, mutual coupling, polarization

1. Introduction

In this research work we analyze and quantize the effect of polarized electromagnetic waves on the performance of adaptive antenna arrays, and we compare the performance of single-dipole adaptive arrays with the performance of cross-dipole adaptive arrays, under similar operating conditions. The effect of polarized incoming desired and undesired signals will be thoroughly investigated against different variables, including angles of arrivals (DOAs) of the incoming signals, input desired signal to noise ratio (SNR), input interference to noise ratios (INRs), number of interference signals, number of the antenna elements in the array, and the extent of pointing error of the main steered beam of the array. This paper also includes experimental and simulation results to illustrate the impact of these parameters on the performance of steered beam adaptive arrays.

In order to build a signal model for this system, we assume that the elements of the antenna array are dipoles separated by uniform distances Δy. Fig. 1 depicts the geometry of a single-dipole antenna array, while Fig. 2 depicts the geometry of a cross-dipole antenna array, where θ and ϕ are the angles of the polar coordinate system. Also, it is assumed that the desired signal, and M interference signals are impinging on the antenna array, such that (θ_d, ϕ_d) are the angular coordinates of the arrival angles of the desired signal, and (θ_i, ϕ_i) are the angular coordinates of the arrival angles of the i-th interference signal. Hence, the signal vector X of an N-element array can be expressed as:

$$X = [\bar{x}_1(t), \bar{x}_2(t), \bar{x}_3(t), \ldots, \bar{x}_N(t)] = S_d + \sum_{i=1}^{M} S_{I_i} + S_n\,, \tag{1}$$

where: the vectors of the desired signal, the i-th interference signal impinging of the i-th element of the array, and the white noise signals can be defined, respectively, as:

$$S_d \triangleq [s_{d_1}(t), s_{d_2}(t), \ldots, s_{d_N}(t)]\,, \tag{2}$$

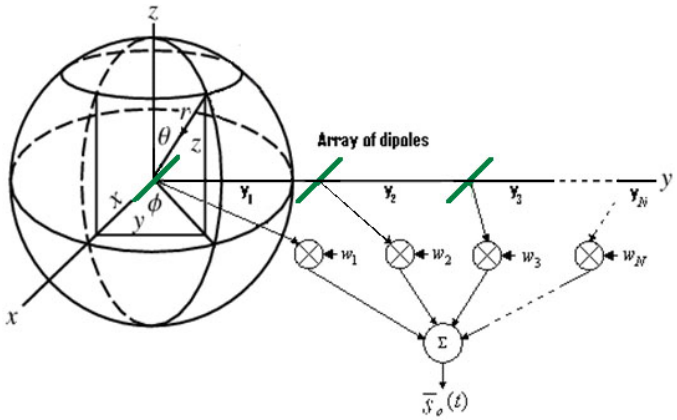

Fig. 1. Geometry of single-dipole antenna array

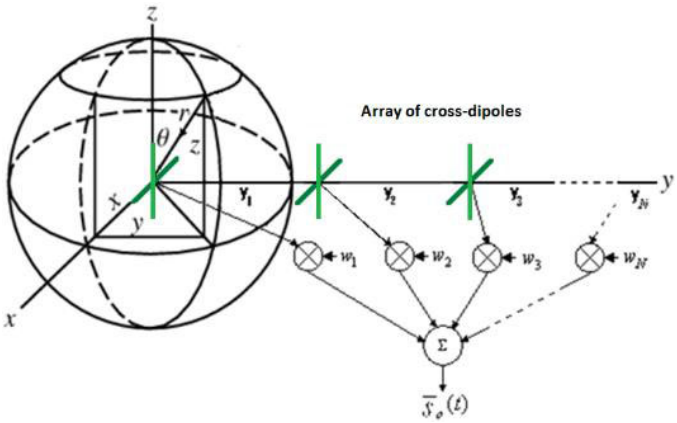

Fig. 2. Geometry of cross-dipole antenna array

$$S_{I_i} \triangleq \left[s_{I_{i1}}(t), s_{I_{i2}}(t), \ldots, s_{I_{iN}}(t)\right], \tag{3}$$

$$S_n \triangleq \left[s_{n_1}(t), s_{n_2}(t), \ldots, s_{n_N}(t)\right]. \tag{4}$$

In this case, we are assuming that all of these signals are randomly polarized electromagnetic waveforms. In order to epitomize the polarization of these signals, we shall make some extra definitions. Firstly, we consider a transverse electro-magnetic (TEM) wave impinging on the antenna array, as depicted in Fig. 1, and Fig. 2. The transverse electric field components of the incoming signal are given by [1, 2]:

$$\overline{E} = E_\phi \hat{\phi} + E_\theta \hat{\theta}, \tag{5}$$

where E_ϕ and E_θ are the electric field components, and they form the polarization ellipse shown in Fig. 3(a), where β represents the orientation angle of the major axis of the polarization ellipse with respect to E_ϕ. To avoid obscurities, the angle β should always be in the range $0 \leq \beta < \pi$, and the magnitude of the ellipticity angle α is given by [1, 2].

$$\alpha = \tan^{-1} A_r, \tag{6}$$

where A_r is the axial ratio defined as:

$$A_r = \frac{\text{minor axis of the polarization ellipse}}{\text{major axis of the polarization ellipse}}. \tag{7}$$

The ellipticity angle α is considered positive when the rotation of the electromagnetic vector is clockwise, and it is considered negative when the rotation is counterclockwise. Fig. 3(a) shows the situation in which α is positive. However, α should always be in the range $-\pi/4 \leq \alpha < \pi/4$.

Away from a common phase factor, and for a given state of polarization, the components of the electric field with amplitude A, can be expressed as:

$$E_\phi = A \cos \gamma, \tag{8}$$

$$E_\theta = A \sin \gamma e^{j\eta}, \tag{9}$$

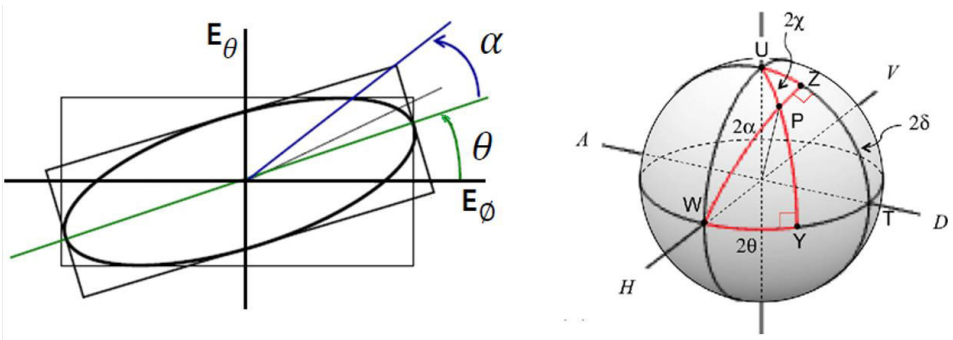

(a) (b)

Fig. 3. (a) polarization ellipse; (b) Poincare sphere

where γ and η are related to α and β by

$$\cos 2\gamma = \cos 2\alpha \cdot \cos 2\beta, \tag{10}$$

$$\tan \eta = \tan 2\alpha \cdot \cos 2\beta. \tag{11}$$

The Poincare sphere depicted in Fig. 3(b) can be used to illustrate the relationship between the angular variables α, β, γ, and η [1, 2]. The point M on the Poincare sphere represents a state of polarization, the point H represents the horizontal polarization, while 2γ, 2β, and 2α form the sides of a spherical right triangle. Side 2β is orthogonal to side 2α, and η is the angle between the sides 2γ and 2β. However, when $\alpha = 0$, the signal will be linearly polarized; in this special case the point M will lie on the equator of the sphere. Additionally, when $\beta = 0$, E_θ will be zero, and E_ϕ will be nonzero, and hence the electromagnetic wave will be horizontally polarized. Point H on the sphere in Fig. 3(b), corresponds to this situation [1, 2].

Consequently, the desired signal can be fully identified by its angle of arrival (θ_d, ϕ_d), its polarization ellipticity angle α_d, its orientation angle β_d, and its amplitude A_d (where A_d is the value of A in Eqs. (8), (9)). Therefore, the desired signal can be completely identified by the parameters $(\theta_d, \phi_d, \alpha_d, \beta_d, A_d)$. Likewise, the i-th interference signal can be completely identified by the parameters $(\theta_i, \phi_i, \alpha_i, \beta_i, A_i)$.

2. Signal model

2.1. Ideal signal model

In this model we assume that the elements of the antenna array are half wave length dipoles, and the mutual coupling between dipoles is initially ignored. Hence, the outputs of the vertically and horizontally positioned dipoles shown in Fig. 1, and Fig. 2 are proportional to the z and x components of the electric field, respectively. a randomly polarized received signal, with electric field components E_ϕ and E_θ will have the following x, y, z components:

$$\begin{aligned}(E_\theta \sin\theta)\,\hat{z}\overline{E} &= E_\phi\hat{\phi} + E_\theta\hat{\theta} = \\ &= \left(E_\theta \cos\theta\cos\phi - E_\phi \sin\phi\right)\hat{x} + (E_\theta \cos\theta \sin\phi - \cos\phi)\,\hat{y} - (E_\theta \sin\theta)\,\hat{z}.\end{aligned} \tag{12}$$

Using the definitions of E_ϕ and E_θ in Eq. (8) and Eq. (11), the electric field components can be given by

$$\begin{aligned}\overline{E} = A[&\left(\sin\gamma\cos\theta\cos\phi e^{j\eta} - \cos\gamma\sin\phi\right)\hat{x} + \\ &+ \left(\sin\gamma\cos\theta\cos\phi e^{j\eta} + \cos\gamma\cos\phi\right)\hat{y} - \left(\sin\gamma\sin\theta e^{j\eta}\right)\hat{z}].\end{aligned} \tag{13}$$

On the other hand, the radiation pattern of the individual dipoles of length l, shown in Fig. 1, can be expressed as [6]:

$$V = \eta\frac{|I_0|^2}{8\pi^2}\left[\frac{\cos(kl/2)\cos\phi - \cos(kl/2)}{\sin\phi}\right]^2, \tag{14}$$

where: η is the characteristic impedance ($\eta \approx 377\ \Omega$ for free space), $|I_0|$ is the amplitude of the current, and $k = 2\pi f\sqrt{\mu_0\varepsilon_0}$, where μ_0 and ε_0 are the permeability and permittivity of free space. By taking into consideration the time delay, space, and phase factors of an incident narrowband clockwise wave on the antenna array incoming from the direction of the main beam ($\theta = \theta_{\max},\ \phi = 90^\circ$), the signal will produce the following signal vector X (previously defined in Eq. (1)):

$$X = VU \cdot \left[1, e^{-jk\Delta z \sin\theta_{\max}} e^{-j2k\Delta z \sin\theta_{\max}}, \ldots, e^{-j(N-1)k\Delta z \sin\theta_{\max}}\right], \tag{15}$$

where: $\theta_{\max}$ is the direction of the main beam of the array, V is given in Eq. (14), and U is given by

$$U = A\left(\left(\sin\gamma\cos\theta\cos\phi e^{j\eta} - \cos\gamma\sin\phi\right) - \left(\sin\gamma\sin\theta e^{j\eta}\right)\right) e^{j(\omega_c t+\psi)}. \tag{16}$$

In this equation, ω_c is the center frequency of the spectrum of the narrowband signal, and ψ is the signal phase at the origin of the coordinate system at $t = 0$ [3–5]. The output of the i-th antenna element is a random complex process, and it is denoted by $\bar{x}_i(t)$. In the beam forming network shown in Fig. 1, and Fig. 2, each individual output of the antenna elements is multiplied by its corresponding complex weight w_i, and combined with the other outputs to produce the total output of the array $\bar{s}_o(t)$.The steady-state weight vector of the array which maximizes its output SINR can be expressed as:

$$w = [w_1, w_2, w_3, \ldots, w_N]^T = [I_N + K\Phi]^{-1}\ \overline{w}_o\,, \tag{17}$$

where: $\Phi = EX^*X^T$ is the covariance matrix, $\overline{w}_o = [w_{10}, w_{20}, w_{30}, \ldots, w_{N0}]^T$ is the array steering weight vector, I_N is the identity matrix, K is the array feedback loop gain, * is the complex conjugate, T is the matrix transpose, and E denotes the mean of the random process.

Hence, the overall output of the array can be given as:

$$\overline{S}_o(t) = X^T w = U\left[w_1 + w_2 e^{-j\mu_1} + w_3 e^{-j\mu_2} + \ldots w_N e^{-j\mu_{N-1}}\right] e^{j(\omega_c t+\psi)}, \tag{18}$$

where

$$\mu_i \triangleq i\Delta z k\cos\theta_{\max}\,. \tag{19}$$

The quiescent sensitivity pattern of the antenna array will yield a maximum output SINR when

$$w_1 = w_2 e^{-j\mu_1} = w_3 e^{-j\mu_2} = \ldots = w_N e^{-j\mu_{(N-1)}}. \tag{20}$$

Therefore, for a given $\theta_{\max}$, $\overline{w}_o$ is typically chosen as:

$$\overline{w}_o = \left[e^{-j\mu_{(N-1)}}, \ldots, e^{-j\mu_2}, e^{-j\mu_1}, 1\right]^T. \tag{21}$$

Consequently, the steering vector $\overline{w}_o$ expressed in Eq. (21), can be used to evaluate the steady-state weight vector w, as described in Eq. (17).

2.2. Practical signal model

In this model, the effect of mutual coupling between the dipole antenna elements of the array will be taken into consideration. As previously explained, Fig. 1 illustrates the geometry of single-dipole antenna array, while Fig. 2 illustrates the geometry of a cross-dipole antenna

array. The outputs of the individual antenna elements are multiplied by complex weights, and then combined to produce the overall output of the array [7]. In this arrangement, the antenna array elements are subjected to mutual coupling, which has a significant impact on the array performance; in terms of lowering its output SINR.

The mutual coupling matrix C can be employed to characterize the mutual coupling between the antenna elements [8–12] and it can be expressed as:

$$C = (Z_A + Z_T)(Z + Z_T I_N)^{-1}, \tag{22}$$

where: Z_A represents the impedance of the isolated antenna (for $\lambda/2$ dipole, $Z_A = 73 + j42.5\ \Omega$), Z_T is the input impedance of the receiving system, and it is selected such that $Z_T = Z_A^*$, in order to obtain full impedance matching between the antenna and the receiving system, I_N is the $N \times N$ identity matrix, and Z is the mutual coupling impedance, which is given by

$$Z = \begin{pmatrix} Z_A & Z_{12} & \cdots & Z_{1N} \\ Z_{21} & Z_A & \cdots & Z_{2N} \\ \vdots & \vdots & \ddots & \vdots \\ Z_{N1} & Z_{N2} & \cdots & Z_A \end{pmatrix}, \tag{23}$$

where Z_{mn} represents the mutual coupling impedance between the m-th and n-th elements.

For dipoles of length l, Z can be evaluated using the method of induced electromagnetic force (EMF), that can produce an analytical expression for Z_{mn}. For the geometry of parallel dipoles of equal lengths $l \leq \lambda/2$, shown in Fig. 1, the mutual impedance between any two dipoles Z_{mn} (where $1 \leq m, n \leq N$) can be expressed as:

$$Z_{mn} = 30\left[0.5772 + \ln(2\beta l) - C_i(2\beta l)\right] + j\left[30 S_i(2\beta l)\right], \quad \text{for } m = n, \tag{24}$$

$$Z_{mn} = 30\left[2C_i(u_0) - C_i(u_1) - C_i(u_2)\right], \\ j\left[30\left(2S_i(u_0) - S_i(u_1) - S_i(u_2)\right)\right] \quad \text{for } m \neq n, \tag{25}$$

where:

$$\beta = \frac{2\pi}{\lambda}, \quad u_0 = \beta d_h, \quad u_1 = \beta\left(\sqrt{d_h^2 + l^2} + l\right), \quad u_2 = \beta\left(\sqrt{d_h^2 + l^2} - l\right)$$

and

$$d_h = \sum_{i=m-1}^{n-1} y_i$$

is the distance between the m-th and n-th dipoles. $S_i(u)$ and $C_i(u)$ are the sine and cosine integrals, respectively, and are given as:

$$S_i(u) = \int_{\infty}^{u} (\sin(x)/x)\, \mathrm{d}x, \qquad C_i(u) = \int_{\infty}^{u} (\cos(x)/x)\, \mathrm{d}x.$$

By examining the radiation/sensitivity pattern of the individual dipoles given in Eq. (14), and the analytical expressions of the mutual coupling between the dipole antennas, expressed in

Eqs. (24), (25), it can be concluded that the mutual coupling between the two elements of the crossed dipoles is much less than that of parallel dipoles, and hence it can be ignored.

Typical applications of adaptive antenna arrays, include their usage in base stations of cellular mobile communication systems, where the mobile transceivers are expected to be randomly distributed around the base stations in the $x-y$ plane (i.e. $\phi = 90°$). Therefore, it can be assumed that all signals lie in the $x-y$ plane [13–19].

In this arrangement, the conditions of line-of-sight signal propagation apply, with one desired signal, and M interference signals. This situation is applicable to rural, or suburban cellular environment, or even it could be applicable to satellite-land communication systems.

When mutual coupling between the parallel antenna elements shown in Fig. 1 and Fig. 2 is taken into consideration, the signal vector X defined in Eq. (1), can be rewritten as:

$$X = CS_d + \left(\sum_{i=1}^{M} CS_i\right) + CS_n\,, \tag{26}$$

where C is the mutual coupling matrix expressed in Eq. (22).

3. Experimental and simulation results

A proof of concept experiment was carried out to gage the radiation pattern of an 8-element adaptive antenna array, and compared the measurement results with the simulation results of the radiation pattern, under the same operating conditions. In this experiment, an antenna array formed of eight wire dipoles has been designed and implemented, as shown in Fig. 4(a), and placed in an anechoic room as shown in Fig. 4(b), where the operating frequency of the system is 2.5 GHz.

The complex weights (attenuators, and phase shifts) of the antenna array are obtained by connecting the dipoles to coaxial cable sections with different lengths stripped off an outer conductor, and to a number of fixed attenuators. The lengths of the coaxial cable sections are determined based on the required phase shift for each element of the array, and the number of fixed attenuators depends on the amount of attenuation required for each antenna element. Then, the attenuated and phase shifted signals of the antenna elements are combined into an 8:1 power combiner as shown in Fig. 4, to produce the overall output of the array.

In order to minimize the return loss between the antenna elements and the coaxial cables, the lengths of the dipoles were selected to be 0.45λ (= 54 mm). It is found that the measured return loss for each antenna element is less than 13 dB, which lies within the acceptable value of the return loss (less than 12 dB). In this experiment, the 8-antenna array elements have a uniform spacing of ($\lambda/2$ = 60 mm) as depicted in Fig. 4(a).

The transmitter used in this experiment is a horn antenna located at a distance of 3 meters from the antenna array with a transmitting frequency of 2.5 GHz. a stepping motor is used to rotate the antenna array shown in Fig. 4, around its center at steps of 1.2°, while the output of the 8-port power combiner is being measured.

Fig. 5(a) depicts the simulated radiation pattern of the antenna array, where mutual coupling is ignored, while Fig. 5(b) shows the simulated pattern of the array, taking mutual coupling into

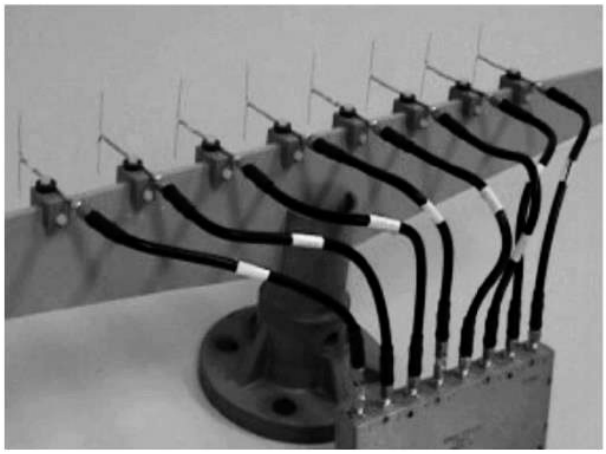

(a)

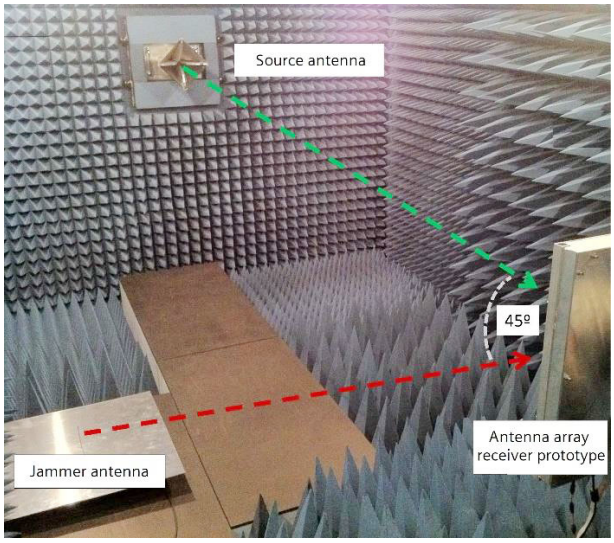

(b)

Fig. 4. (a) photograph of the experiment prototype showing the 8-element antenna array, uniformly spaced by $\lambda/2$; (b) anechoic chamber

consideration. On the other hand, Fig. 5(c) depicts the experimentally measured radiation pattern of the antenna array, under the same operating conditions.

The return loss is defined as $RL = 20\log_{10}|S_{11}|$, where the scattering parameter S_{11} is measured by the network analyzer in microwave laboratories of The University of Queensland.

It can be clearly observed that a good match exists between the simulation results shown in Fig. 5(b), where the mutual coupling is taken into consideration, and the experimental results

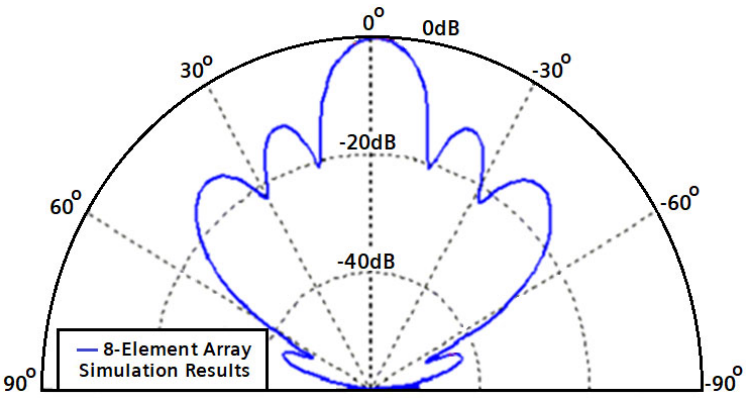

(a)

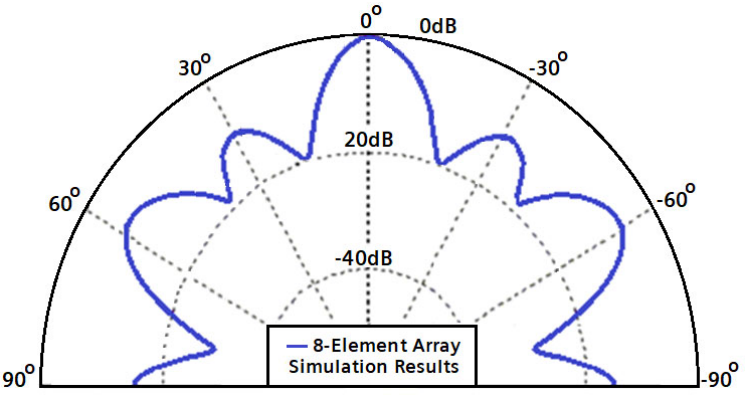

(b)

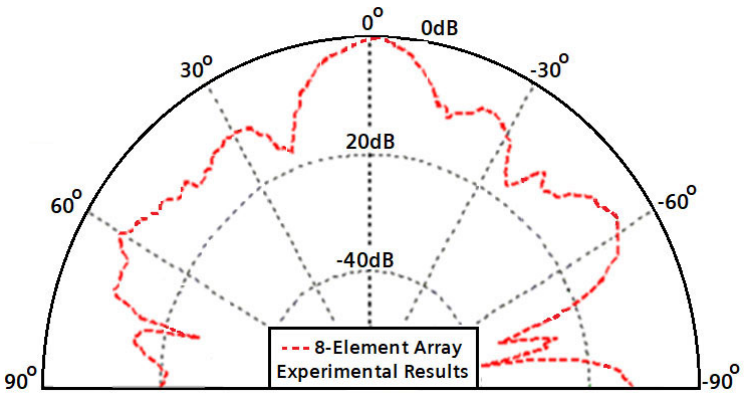

(c)

Fig. 5. Simulation and experimentally measured radiation patterns of the antenna array (depicted in Fig. 4): (a) simulated pattern (mutual coupling is ignored, or compensated); (b) simulated pattern (with mutual coupling); (c) experimentally measured radiation pattern

shown in Fig. 5(c). However the slight discrepancies between the experimentally measured radiation pattern in Fig. 5(c), and the simulated radiation pattern in Fig. 5(b) are caused by a number of factors; such as (1) the inaccuracy in the attenuators used in the array, (2) the errors in phase shifters due to inaccuracy in the lengths of the coaxial cables (where every 1 mm of the cable length provides a phase shift of 3°), and (3) the manufacturing faults of the individual dipoles. Fig. 6 shows the output SINR of an 8-single dipole uniformly spaced antenna array, versus the pointing error θ_{perr} of the main beam with respect to the DOA of the desired signal (where, $\theta_{\text{perr}} = \theta_d - \theta_{\max}$).

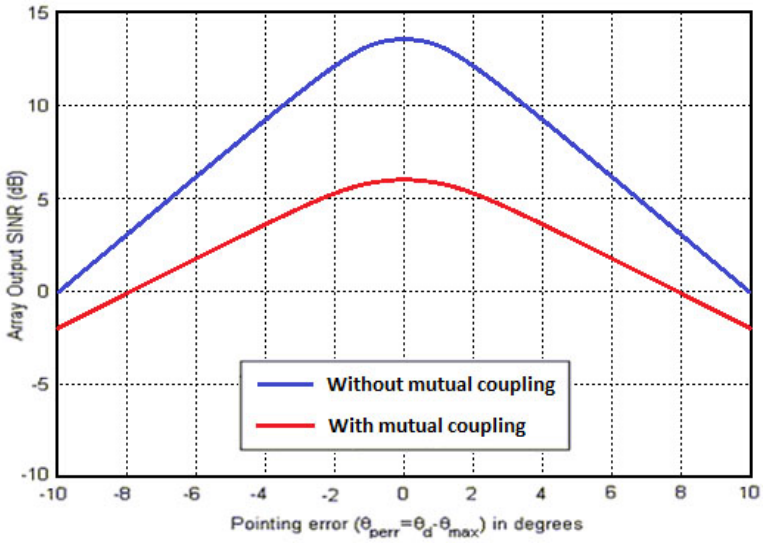

Fig. 6. SINR vs. (θ_{perr}) for single-dipole array, with and without mutual coupling; SNR = 10° dB, $\theta_d = 0°$; no interference

In this case, we assumed that a 10dB-SNR desired signal is incident on the single-dipole array shown in Fig. 1, where the direction of the main beam is $\theta = 90°$, $\phi = 90°$, and the polarization of the desired signal is linear (i.e. $\alpha_d = 0°$).

Fig. 6 depicts that the output SINR of the array has a maximum value, when the pointing error of the main beam of the array is 0°. Also, it can be concluded that the mutual coupling reduces the output SINR of the array, and therefore, it has a negative effect on its performance.

Assuming the direction of arrival of the desired signal is well known (i.e. the pointing error $\theta_{\text{perr}} = \theta_d - \theta_{\max} = 0°$); Fig. 7(a) illustrates the output SINR when the desired signal is linearly polarized, while Fig. 7(b) shows the output SINR when the desired signal is circularly, or elliptically polarized. It can be seen that the horizontally polarized desired signal gives the best performance of the array, because the electric field $\overline{E}$ lies along the x-axes (i.e. in parallel with the dipoles).

Fig. 8 depicts the output SINR versus the input interference to noise ratio (INR) per antenna element, for various types of polarization of the interference signal. Here, both the de-

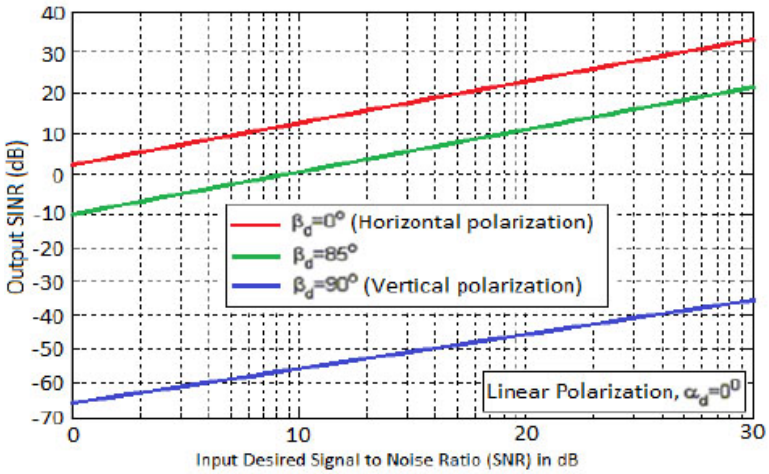

(a)

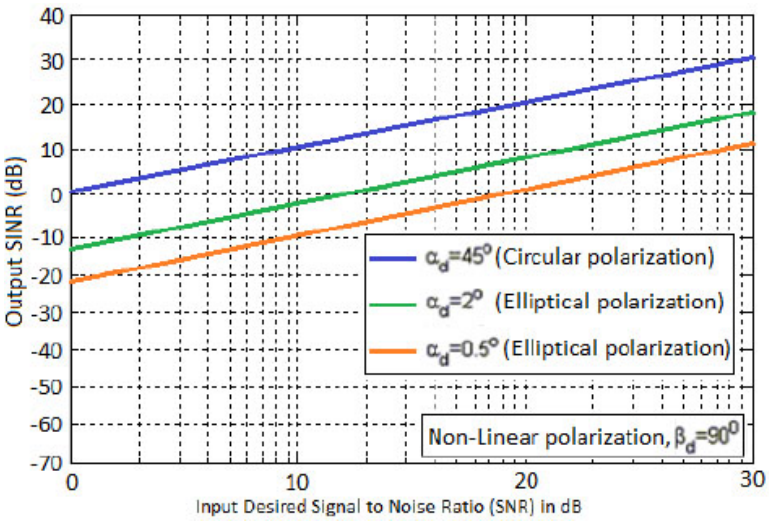

(b)

Fig. 7. Output SINR vs. input SNR/element for single-dipole array, no interference: (a) $\alpha_d = 0°$; (b) $\beta_d = 90°$

sired and interference signals have incident angles of $\theta_d = \theta_i = 0°$, and the pointing error $\theta_{\text{perr}} = (\theta_d - \theta_{\max}) = 0°$.

It can be seen that the vertically polarized interference signal has no effect on the array, while the horizontally polarized interference signal has the most negative impact on the array, as its electric field is in parallel with the dipole antennas. In the latter case the output SINR decreases drastically as INR increases.

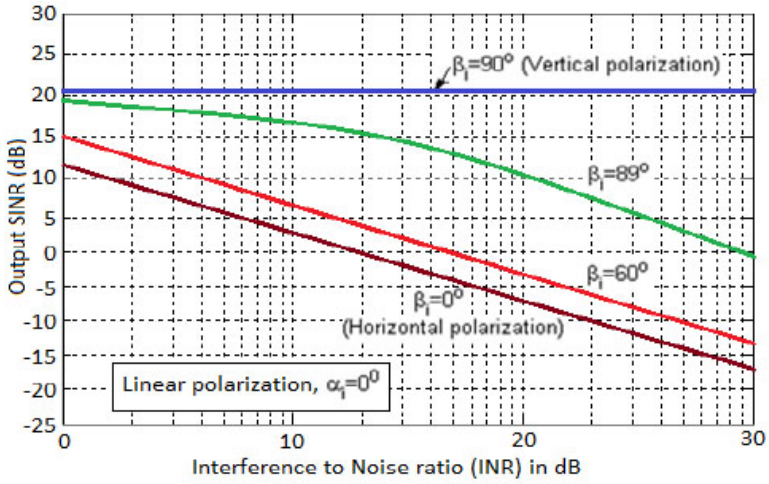

(a)

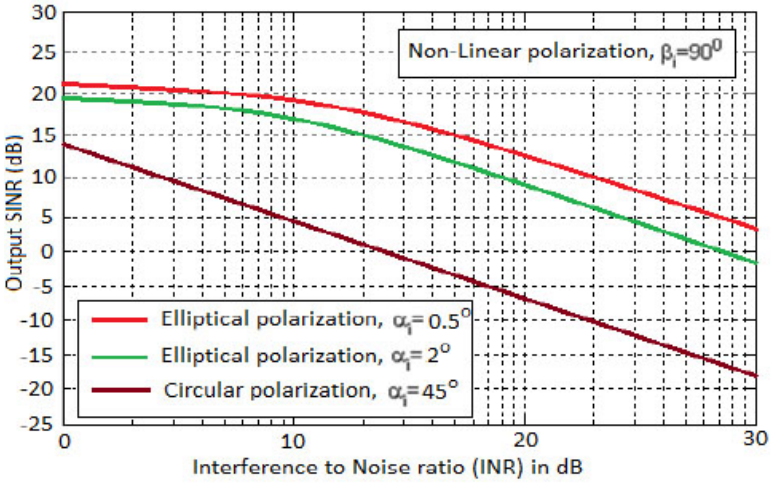

(b)

Fig. 8. Output SINR vs. INR/element for single-dipole array: (a) SNR = 20 dB, $\theta_d = 0°$, $\theta_i = 0°$, $\alpha_d = 0°$; b) $\beta_d = 90°$

By comparing these results with those in Fig. 7, it can be concluded that if the polarization of the desired signal and its DOA are known, this information can be employed to get the best performance of the array. On the other hand, if the polarization of the desired signal is completely unknown, cross-dipole adaptive arrays (shown in Fig. 2) can be used to improve the performance of the antenna array. This arrangement makes the performance of the array independent of the polarization of the desired and interference signals, hence it gives a reasonable output SINR, regardless of the polarization of the desired and interference signals, as can be clearly concluded

from Fig. 9 and Fig. 10. By comparing the Figures corresponding to cross-dipole adaptive arrays (i.e. Fig. 9, and Fig. 10) to the Figures corresponding to single-dipole arrays (i.e. Fig. 7, and Fig. 8), it can be concluded that, in general, cross-dipole adaptive antenna arrays exhibit better performance than single-dipole adaptive antenna arrays in presence of randomly polarized signals. However, single-dipole adaptive arrays give better performance, if the polarization of the desired signal is known, and employed to achieve this goal.

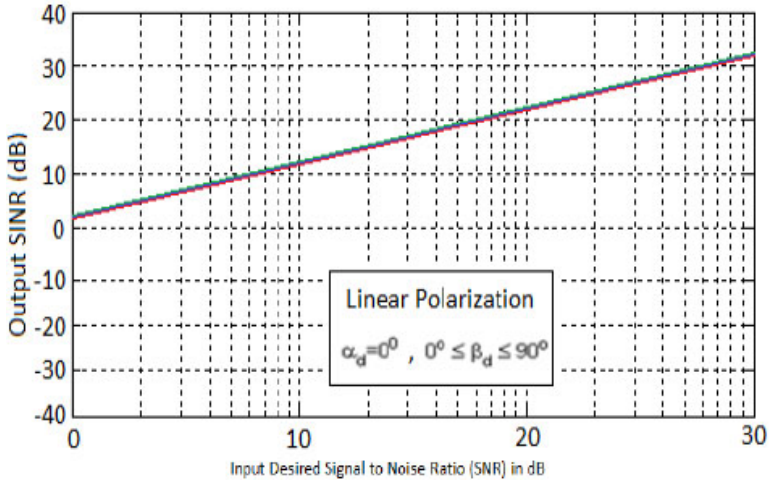

(a)

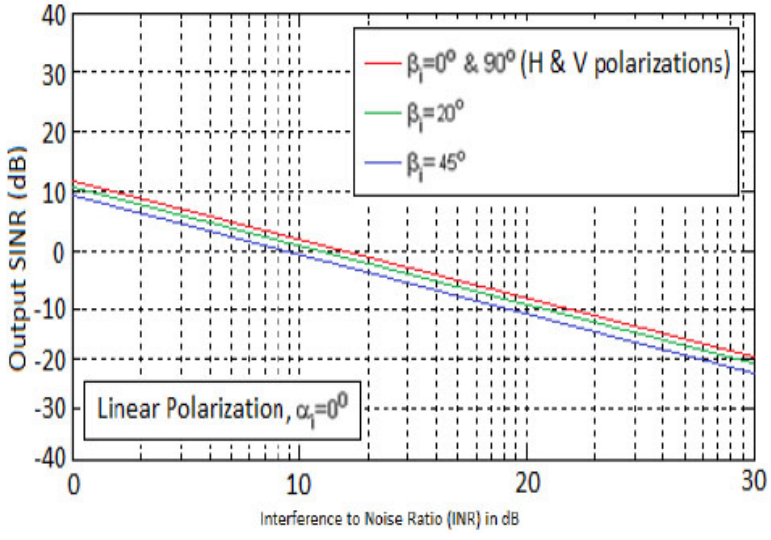

(b)

Fig. 9. Output SINR vs. input SNR/element for cross-dipole array, no interference: (a) $\alpha_d = 0°$; (b) $\beta_d = 90°$

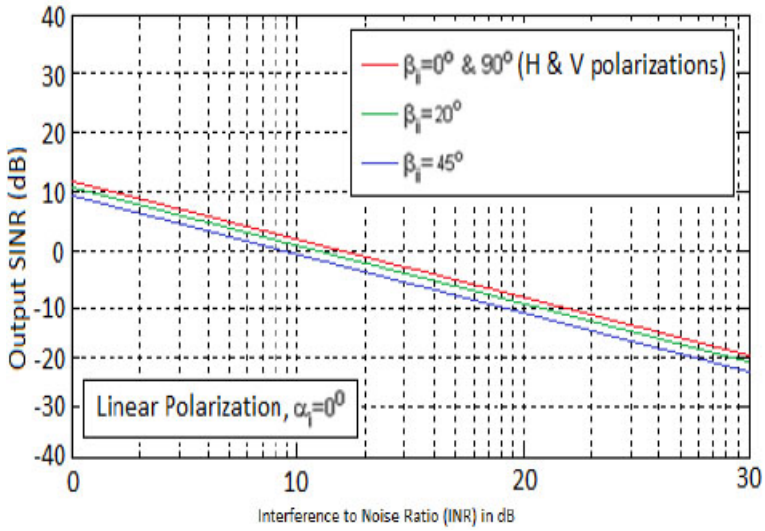

(a)

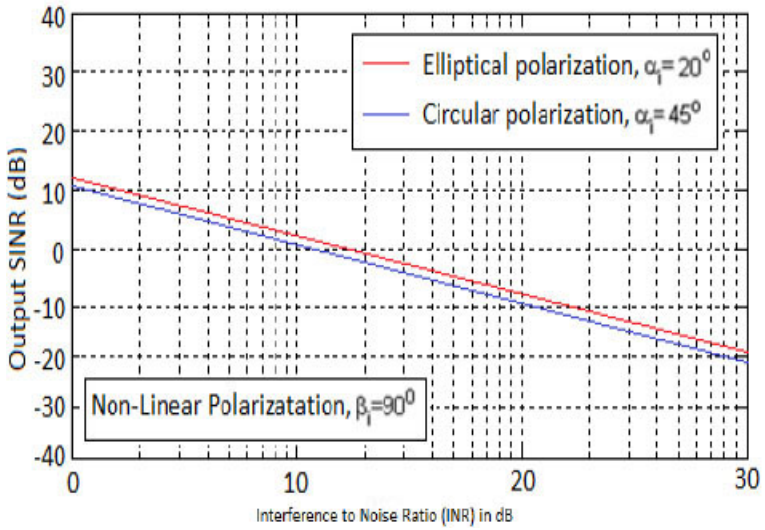

(b)

Fig. 10. Output SINR vs. INR/element for cross-dipole array: (a) SNR = 20 dB, $\theta_d = 0°$, $\theta_i = 0°$, $\alpha_d = 0°$, (b) $\beta_d = 90°$

4. Conclusions

In this paper, we analyzed, and presented the effect of polarized desired, and interference signals on the performance of uniformly-spaced adaptive antenna arrays. It was found that the knowledge of the polarization of the desired signal, and its direction of arrival, can be employed to

get the best outcome (i.e. highest SINR) from the single dipole adaptive antenna array. However, if the polarization parameters of the desired signal are completely unidentified, cross-dipoles antenna elements can be used to achieve this goal.

References

[1] Jones J.A., D'Addario A.J.J., Rojec B.L., Milione G., Galvez E.J., *The Poincare-sphere: approach to polarization: Formalism and new labs with Poincare beams*, accessed March (2018), DOI: 10.1119/1.4960468.

[2] Compton R.T., *On the performance of a polarization sensitive adaptive array*, IEEE Transactions on Antennas Propagation, vol. 29, pp. 718–725 (1981).

[3] Hum S.V., Carrier J., *Reconfigurable reflect-arrays and array lenses for dynamic antenna beam control: a review*, IEEE Transactions on Antennas Propagation, vol. 62, no. 1, pp. 183–198 (2014).

[4] Florencio R., Encinar J.A., Toso G., *Reflect-array antennas for dual polarization and broadband telecom satellite applications*, IEEE Transactions on Antennas Propagation, vol. 63, no. 4, pp. 1234–1246 (2015).

[5] Mohammad Hashim Dahri, Jamalueddin M., *Polarization Diversity and Adaptive Beam-steering for 5G Reflect-arrays: a Review*, IEEE Access, vol. 6, pp. 19452–19465 (2018).

[6] Constantine Balanis, *Antenna Theory, Analysis and Design*, John Wiley and Sons Inc., 4th edition (2016).

[7] Compton R.T. Jr., *Adaptive Antennas, Concepts and Performance*, Prentice-Hall, New Jersey, pp. 45–110 and 355–389 (1988).

[8] Svantesson T., *Estimation and Modelling of mutual coupling in a uniform linear array of dipoles*, in proc. ICASSP'99, Phoenix, AZ, pp. 2961–2964 (1999).

[9] Amin Al Ka'bi, *Performance of Adaptive Antennas in Presence of Polarized Electromagnetic Signals*, Telecommunications and Radio Engineering, Bentham Science Publisher, vol. 79, iss. 4, pp. 291–304, ISSN:0040-2508 (2020), DOI: 10.1615/telecomradeng.v79.i4.30.

[10] Ayodele Sunday Oluwole, Viranjay M. Srivastava, *Smart Antenna for Wireless Communication Systems using Spatial Signal Processing*, Journal of Communications, vol. 12, no. 6, pp. 328–339 (2017), DOI: 10.12720/jcm.12.6.328-33.

[11] Amin Al Ka'bi, Bialkowski M.E., Homer J., *On the performance of adaptive antenna array in mobile fading environment*, 16th International Conference on Microwaves, Radar and Wireless Communications, MIKON (2006), DOI: 10.1109/MIKON.2006.4345219.

[12] Compton R.T., *On the performance of a polarization sensitive adaptive array*, IEEE Transactions on Antennas Propagation, vol. 29, pp. 718–725 (1981).

[13] Kwan Hyeong Lee, Tae Jun Cho, *Performance Analysis of Noise Signal Reduction Using Novel MUSIC Method of Adaptive Arrays*, Journal of Communications, vol. 12, no. 6, pp. 347–352 (2017), DOI: 10.12720/jcm.12.6.347-352.

[14] Amin Al-Ka'bi, Bialkowski M.E., John H., *Performance Comparison between Uniformly and Non-Uniformly Spaced Adaptive Antennas with Respect to Tolerance to Pointing Errors*, Journal of Microwave and Optical Technology Letters, ISSN: 1098-2760, vol. 48, no. 11 (2006), DOI: 10.1002/mop.21904.

[15] Bahar Ghaderi, Naser Parhizgar, *Resource allocation in MIMO systems specific to radio communication*, Archives of Electrical Engineering, vol. 68, no. 1, pp. 91–100 (2019), DOI: 10.24425/aee.2019.125982.

[16] Amin H. Al Ka'bi, *Effect of Polarization on the Performance of Adaptive Antenna Arrays*, Journal of Communications, vol. 15, no. 9, pp. 661–668 (2020), DOI: 10.12720/jcm.15.9.661-668.

[17] Naser Parhizgar, *A new mutual coupling compensation method for receiving antenna array-based DOA estimation*, Archives of Electrical Engineering, vol. 67, no. 2 (2018), DOI: 10.24425/119650.

[18] Amin Al-Ka'bi, Bialkowski M.E., John H., *Mitigation of Multipath Propagation with the Use of a Non-Uniform Spaced Adaptive Array Antenna*, IEEE Antenna and Propagation Society (AP-S) International Symposium and USNC/URSI National Radio Science Meeting, Washington DC, vol. 2B, pp. 56–59, 3–8 July (2005), DOI: 10.1109/APS.2005.1551934.

[19] Mohamed Deriche, Amin Al-Ka'bi, *On the performance of adaptive steerable antenna arrays in communication applications*, IEEE 1st International Conference on Computers, Communications, and Signal Processing, 2005 (CCSP 2005), Kuala Lumpur, Malaysia, P-ISBN: 978-1-4244-0011-9, pp. 15–20 (2005), DOI: 10.1109/CCSP.2005.4977150.